ELSEVIER

Journal of Organometallic Chemistry 632 (2001) 75–84

Journal of Organometallic Chemistry

www.elsevier.com/locate/jorganchem

Biscyclopentadienyl Group 6 metal complexes as metalloligands in the synthesis of heterobimetallic species. Crystal structures of new thiolato-bridged molybdenum(IV)–copper(I) complexes

Alberto R. Dias [a,*], M. Helena Garcia [a,b,*], Maria J. Villa de Brito [a,b], Adelino Galvão [a]

[a] *Centro de Química Estrutural, Instituto Superior Técnico, Av. Rovisco Pais, 1049-001 Lisbon, Portugal*
[b] *Faculdade de Ciências da Universidade de Lisboa, DQB, R. Ernesto de Vasconcelos, 1749-016 Lisbon, Portugal*

Received 20 February 2001; accepted 24 May 2001

On the occasion of Professor Alberto R. Dias' 60th birthday

Abstract

Heterobimetallic complexes of the form $[M(\eta^5\text{-}C_5H_5)_2(\mu\text{-}SR)_2CuL_n][BF_4]$ where M = Mo, R = Ph, L = PPh_3, $n = 2$ (**1**); M = W, R = Ph, L = PPh_3, $n = 2$ (**2**); M = Mo, R = Ph, L = PPh_3, $n = 1$ (**3**); M = W, R = Ph, L = PPh_3, $n = 1$ (**4**); M = Mo, R = Ph, L = py, $n = 1$ (**5**); M = Mo, R = ^{t}Bu, L = PPh_3, $n = 1$ (**6**); $[Mo(\eta^5\text{-}C_5H_5)_2(\mu\text{-}SPh)_2CuNCMe]_2[BF_4]_2$ (**7**); and the trinuclear compound $[\{Mo(\eta^5\text{-}C_5H_5)_2(\mu\text{-}SPh)_2\}_2Cu][BF_4]$ (**8**) have been prepared and characterised. The molecular structures of **1**, **3** and **7** have been determined by single-crystal X-ray diffraction studies. The molybdenum atoms exhibit the usual bent metallocene structure with a distorted tetrahedron around each metal atom, similar to that of the free metalloligand. The coordination around the copper is tetrahedral in **1** and in the dimer **7**, and trigonal distorted in **3**. The MoS_2Cu core is almost planar in **1**, with an angle of 177.3° between the MoS_2 and the CuS_2 planes; this angle is 154.2° for **3**, 146.2 and 149.4° for **7**, and in the Cu_2S_2 core of the dimer the folding angle is 166.1°. The large angles at the sulphur atoms, the acute angles at the metals, the Mo–Cu distances of 4.011 Å (**1**), 3.664 Å (**3**), 3.653 and 3.649 Å (**7**) and the Cu–Cu distance of 3.147 Å are consistent with the absence of direct metal–metal interactions.

Keywords: Molybdenum biscyclopentadienyl; Copper; Thiolate-bridged; Binuclear; ELHB

1. Introduction

Recently, considerable interest has been focused on the synthesis and study of early–late heterobimetallic complexes (ELHB) [1], which contain two very different metal centres in one molecule, one from the left-hand side of the transition series and the other from the right-hand side. In such complexes, the greatest modification of reactivity over that of monometallic species is expected. The cooperative behaviour between an electrophilic early metal and an electron-rich late metal can give a novel bimetallic reactivity with potential applications, namely in homogeneous catalysis, in the activation of polar molecules. In addition, these complexes have been studied in order to get a better understanding of the phenomenon of 'strong metal-support interactions (SMSI)' often seen in heterogeneous catalysis [2].

Bent metallocene derivatives of general formula $[M(\eta^5\text{-}C_5H_5)_2(SR)_2]$ (M = early transition metal; R = alkyl or aryl) have often been used as chelating ligands to prepare binuclear complexes, due to the high stability of the MCp_2 fragments and the ability of thiolate groups to form M(μ-SR)M′ bridges. Thus, such metalloligands have been extensively used for the synthesis of ELHB systems [1,3–5], especially those involving a d^0 early metal and a d^{10} late transition metal [1a,1b,4,5]. These species have attracted additional interest, due to the nature of the dative ($d^{10} \rightarrow d^0$) interaction between metals.

* Corresponding authors. Tel.: +351-21-8419317; fax: +351-21-8464455.
E-mail address: lena.garcia@ist.utl.pt (M.H. Garcia).

0022-328X/01/$ - see front matter
PII: S0022-328X(01)01047-6

As part of our current interest in the reactivity of molybdenum and tungsten biscyclopentadienyl bisthiolates, we are investigating some of their reactions with $[Cu(NCCH_3)_4]^+$ in different conditions, in order to study the types and nature of the possible interactions between d^2 early metals and d^{10} late transition metals. To our knowledge, no examples of such thiolato-bridged complexes have yet been reported.

According to theoretical studies and conformational aspects of ELHB complexes containing the $[MCp_2(\mu\text{-}SR)_2]$ moiety and an M′Ln fragment [6], the main structural features associated with the metal–metal interactions in such systems are the S–M–S angles of the metalloligands, which depend both on the electron count on the early metal M and on the conformation of the SR ligands (*exo* or *endo*). The *exo* form is preferred by d^2 complexes, which present acute angles at the metals and large M–S–M angles (> 100°), with consequent long M–M′ distances, unlikely to allow metal–metal bond formation. The *endo* form is preferred by d^0 species, which exhibit acute M–S–M′ angles and large angles at M and M′, allowing a closer proximity of the metals, generally enhanced by puckering of the ring. This last situation, observed in Ti(IV) derivatives, is compatible with the formation of metal–metal bonds.

In this paper we report the synthesis of a series of M(IV)–Cu(I) heterobimetallics of the form $[M(\eta^5\text{-}C_5H_5)_2(\mu\text{-}SR)_2CuL_n][BF_4]$, with M = Mo(IV)/W(IV), R = Ph or ^{t}Bu, L = PPh_3, NCMe or pyridine, and $n = 1$ or 2. The results of these studies, which confirm the absence of direct Cu(I)→Mo(IV)/W(IV) interactions, are discussed and compared with those found for the Ti(IV)–Cu(I) analogues [5a,5b,5c], whose structural features are consistent with the presence of Cu→Ti dative interactions.

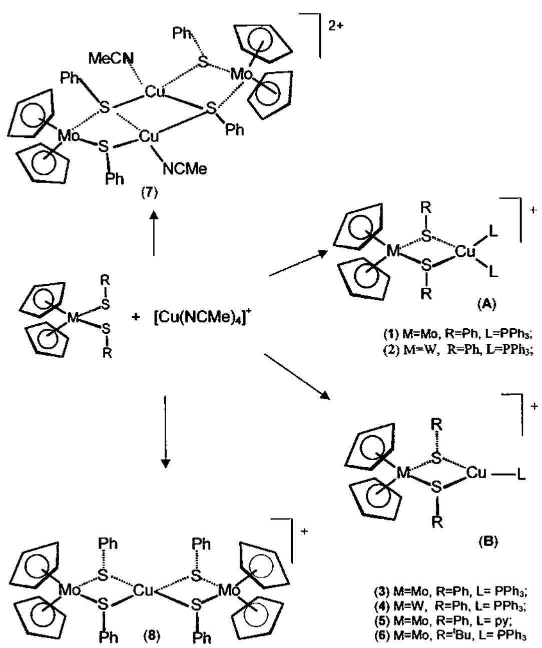

Scheme 1.

2. Results and discussion

2.1. Chemical studies

Addition of the brown–orange metalloligands $[M(\eta^5\text{-}C_5H_5)_2(SR)_2]$ (M = Mo, W; R = Ph, ^{t}Bu) to THF solutions containing $[Cu(NCCH_3)_4][BF_4]$ and either one or two equivalents of triphenylphosphine or pyridine results in a rapid colour change from orange to dark red. Concentration of the solution and slow addition of diethyl ether or recrystallisation by slow diffusion of diethyl ether into acetone solutions of the products causes, in most cases, precipitation of orange or red crystalline solids.

^{1}H-NMR integrations, combustion analysis and molar conductivities of these products indicate the existence of two main groups of heterobimetallic compounds, according to the number of substituents on the copper atom (Scheme 1). Thus, when two equivalents of PPh_3 were used, complexes **1**–**2** with formulation $[MCp_2(\mu\text{-}SR)_2CuL_2][BF_4]$ (**A**) have been obtained (M = Mo, R = Ph, L = PPh_3, **1**; M = W, R = Ph, L = PPh_3, **2**); when only one equivalent of PPh_3 or pyridine was used, compounds **3**–**6** with formulation $[MCp_2(\mu\text{-}SR)_2CuL][BF_4]$ (**B**), have been produced (M = Mo, R = Ph, L = PPh_3, **3**; M = W, R = Ph, L = PPh_3, **4**; M = Mo, R = Ph, L = py, **5**; M = Mo, R = ^{t}Bu, L = PPh_3, **6**). The proposed **A** and **B** formulations have been confirmed by X-ray diffraction crystallographic studies of complexes **1** and **3**, respectively.

The stoichiometry of the final product seems to be conditioned by steric interactions of the bulky substituents R on sulphur with the ligands L coordinated to copper. In fact, the reactions involving thiolates with the bulky ^{t}Bu groups and PPh_3 always led to the **B** formulation $[MoCp_2(\mu\text{-}S^tBu)_2CuPPh_3]$ (**6**), even when more than two equivalents of the phosphine were used.

^{1}H-NMR spectra in $(CD_3)_2CO$ for each of these products show a singlet between 5.38 and 5.80 ppm, included in the usual region for cyclopentadienyl protons of cationic $MoCp_2$ derivatives. Resonances of the aromatic protons are found, as expected, at lower fields: three multiplets between 9.09 and 7.66 ppm have been assigned to the pyridine protons (**7**); complex multiplets in the region 7.59–7.30 ppm correspond to the protons of the triphenylphosphine ligands (**1**, **2**, **3**, **4** and **6**) and one or two multiplets between 7.39 and 7.01 ppm have been assigned to the phenyl protons of thiolate groups. For compound **6**, a singlet at high field, assignable to the ^{t}Bu protons of the thiolates is located at 1.23 ppm. The ^{31}P-NMR spectra for compounds **1**, **2**, **3**, **4**, and **6** show a singlet with chemical shifts

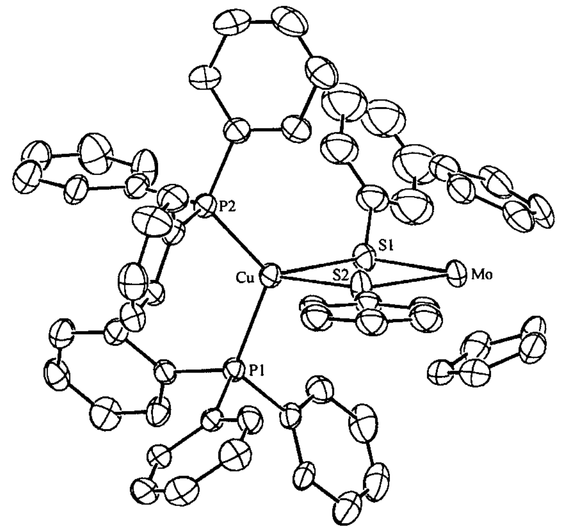

Fig. 1. ORTEP drawing of the cation $[Mo(\eta^5\text{-}C_5H_5)_2(\mu\text{-}SPh)_2Cu(PPh_3)_2]^+$ (**1**). Hydrogen atoms are omitted for clarity. The labelled atoms are symmetry related to their unlabelled counterparts.

between 0.92 and 6.85 ppm, corresponding to the coordinated phosphines.

The IR spectra of the complexes show the typical bands of the coordinated ligands at the following approximate values: Cp, 3100; Ph, 3050; ^{t}Bu, 2900; PPh_3, 520 and py, 1600 cm^{-1}. Also the characteristic broad and strong band assigned to the $[BF_4]^-$ counter-ion was found between 1100 and 1000 cm^{-1}.

These compounds are generally air stable in the solid state but relatively air sensitive in solution. Compounds **1**–**4** (with R = Ph and L = PPh_3) are even stable in solution (acetone) when exposed to air for several days and they have been obtained with ~90% yields. Compound **6** (with R = ^{t}Bu and L = PPh_3) decomposes in THF or acetone after a few days under inert atmosphere and has been prepared with ~40% yield. The pyridine-containing compound **5** is even more air sensitive and has been obtained in lower yield (~30%). Several attempts to prepare other pyridine-containing compounds (with formulation **A**) showed some evidence of their formation, according to the ^{1}H-NMR spectra. However, their full characterisation was difficult, possibly due to ligand exchange reactions at copper(I) on recrystallisation. For the N-containing compounds (**5** and **7**), poor analytical results have been obtained, despite repeated recrystallisations in acetone or THF.

Addition of $[Mo(\eta^5\text{-}C_5H_5)_2(SPh)_2]$ to a colourless acetonitrile solution containing $[Cu(NCCH_3)_4][BF_4]$ gave an orange–red mixture which was refluxed for 2 h. After work up of the reaction product, an orange–red solid was obtained in 75% yield. Slow diffusion of diethyl ether into an acetonitrile solution of the compound caused the precipitation of dark red crystals of the new complex **7**. This product is air stable in the solid state but air sensitive in solution. ^{1}H-NMR spectral integrations and conductivity measurements are consistent with the formulation **B**. An X-ray diffraction analysis of the compound established its formulation as a dimer, $[Mo(\eta^5\text{-}C_5H_5)_2(\mu\text{-}SPh)Cu(NCMe)]_2[BF_4]_2$ (**7**).

The synthesis of the trinuclear compound $[\{Mo(\eta^5\text{-}C_5H_5)_2(\mu\text{-}SPh)_2\}_2Cu][BF_4]$ (**8**) was achieved by slow addition of an acetonitrile solution containing one equivalent of $[Cu(NCCH_3)_4][BF_4]$ to a suspension of two equivalents of $[Mo(\eta^5\text{-}C_5H_5)_2(SPh)_2]$ in the same solvent, in order to provide a higher excess of Mo to Cu in the reaction mixture. After stirring for 1 h at room temperature and work up of the resulting dark red solution, an orange–red crystalline solid was obtained in 85% yield. The ^{1}H-NMR data, elemental analysis and conductivity measurements are consistent with the proposed formulation (Scheme 1). Although an X-ray study of **8** was not carried out (despite several attempts to obtain suitable crystals), its structure is expected to be similar to that of compound **1**, with the Cu(I) atom in a tetrahedral environment and a second $[Mo(\eta^5\text{-}C_5H_5)_2(SPh)_2]$ unit occupying the positions of the two phosphines.

2.2. Crystallographic studies

2.2.1. Crystal structure of $[Mo(\eta^5\text{-}C_5H_5)_2(\mu\text{-}SPh)_2Cu(PPh_3)_2][BF_4]\cdot(Me_2CO)$ ($\mathbf{1}\cdot Me_2CO$)

Single crystals of **1** were obtained by slow diffusion of diethyl ether into an acetone solution of **1**. An X-ray crystallographic study revealed that the crystals were made up of triclinic unit cells, each containing discrete anions and cations, as well as acetone molecules from crystallisation. The cation of **1** is depicted in the ORTEP drawing in Fig. 1. Selected bond distances and angles are given in Table 1.

The Mo atom presents a distorted pseudotetrahedral geometry comprised of two π-bonded cyclopentadienyl rings and two phenyl thiolate ligands. The Cu coordination sphere is also pseudotetrahedral, consisting of the two sulphur atoms of the metalloligand and two phosphorus atoms from the coordinated triphenylphosphines. The MoS_2Cu core of **1** may be considered planar (folding angle = 177.3°) and the phenyl substituents of the thiolates adopt a *cis* disposition, although the S2-containing thiolate group is almost coplanar with the MoS_2Cu core (S1–S2–C21 = 173°; Mo–S2–C21–C22 = 2.5° and S1–Mo–S2–C21 = 177°). The S1-containing thiolate group presents a considerable torsion, characterised by the angles S2–Mo–S1–C11 = 138° and S2–S1–C11 = 145°, as a result of the conformation adopted by the phenyl ring, in order to minimise repulsions with the closer Cp ring

Table 1
Selected bond lengths (Å) and angles (°) for the cations of **1**, **3** and **7**

$[MoCp_2(\mu\text{-}SPh)_2Cu(PPh_3)_2]^+$ (**1**)					
Bond lengths					
Mo–Cp2	1.979	Cu–P(2)	2.270(2)	P1–C(111)	1.809(8)
Mo–Cp1	1.986	Cu–P(1)	2.330(2)	P1–C(121)	1.832(8)
Mo–S(1)	2.509(3)	Cu–S(1))	2.361(2)	P1–C(131)	1.835(8)
Mo–S(2)	2.461(2)	Cu–S(2))	2.576(3)	P(2)–C(231)	1.813(9)
S(2)–C(21)	1.755(9)	S(1)–C(11)	1.754(10)	P(2)–C(211)	1.823(9)
				P(2)–C(221)	1.829(9)
Bond angles					
Cp2–Mo–Cp1	135.6	S(1)–Cu–S(2)	71.96(8)	C(11)–S(1)–Mo	114.8
S(2)–Mo–S(1)	71.57(8)	P(2)–Cu–S(1)	128.25(9)	C(111)–P(1)–C(131)	102.7(4)
Mo–S(2)–Cu	105.51(9)	P(1)–Cu–S(1)	105.54(9)	C(111)–P(1)–C(121)	103.1(4)
Cu–S(1)–Mo	110.87(10)	P(2)–Cu–S(2)	105.97(10)	C(121)–P(1)–C(131)	101.7(4)
C(21)–S(2)–Cu	135.6	P(1)–Cu–S(2)	111.32(9)	C(211)–P(2)–C(221)	102.9(4)
C(21)–S(2)–Mo	118.9	C(11)–S(1)–Cu	122.5	C(231)–P(2)–C(211)	104.2(4)
C(211)–P(2)–Cu	111.4(3)	P(2)–Cu–P(1)	121.59(8)	C(231)–P(2)–C(221)	102.9(4)
C(221)–P(2)–Cu	118.3(3)	C(131)–P(1)–Cu	115.7(3)	C(111)–P(1)–Cu	112.2(3)
		C(231)–P(2)–Cu	115.5(3)	C(121)–P(1)–Cu	119.2(3)
$[MoCp_2(\mu\text{-}SPh)_2Cu(PPh_3)]^+$ (**3**)					
Bond lengths					
Mo–Cp2	1.966	Cu–S(1)	2.338(2)	Cu–P	2.185(2)
Mo–Cp1	1.997	Cu–S(2)	2.245(2)	P–C(51)	1.826(8)
Mo–S(1)	2.509(2)	S(2)–C(21)	1.752(7)	P–C(31)	1.809(8)
Mo–S(2)	2.453(2)	S(1)–C(11)	1.766(8)	P–C(41)	1.825(8)
Bond angles					
Cp2–Mo–Cp1	134.6	Cu–S(2)–Mo	102.42(8)	C(31)–P–Cu	112.2(2)
S(2)–Mo–S(1)	72.52(6)	Cu–S(1)–Mo	98.17(7)	C(41)–P–Cu	108.8(2)
S(2)–Cu–S(1)	79.63(7)	P–Cu–S(2)	148.49(9)	C(51)–P–Cu	121.3(3)
C(11)–S(1)–Cu	116.1	P–Cu–S(1)	127.45(8)	C(31)–P–C(41)	105.3(4)
C(11)–S(1)–Mo	113.2	C(21)–S(2)–Mo	118.7	C(31)–P–C(51)	105.0(4)
		C(21)–S(2)–Cu	127.0	C(41)–P–C(51)	102.9(4)
$[MoCp_2(\mu\text{-}SPh)_2CuNCCH_3]_2^{2+}$ (**7**)					
Bond lengths					
Mo(1)–S(1)	2.506(2)	Mo(1)–Cp(1)	1.97	N(1)–C(1)	1.075(13)
Mo(1)–S(2)	2.514(3)	Mo(1)–Cp(2)	1.98	C(1)–C(2)	1.56(2)
Mo(2)–S(3)	2.491(3)	Mo(2)–Cp(3)	1.98	S(1)–C(11)	1.771(10)
Mo(2)–S(4)	2.534(3)	Mo(2)–Cp(4)	2.00	S(2)–C(21)	1.786(9)
Cu(1)–S(1)	2.436(3)	Cu(2)–S(1)	2.405(3)	N(2)–C(3)	1.08(2)
Cu(1)–S(2)	2.288(3)	Cu(2)–S(3)	2.431(3)	C(3)–C(4)	1.59(2)
Cu(1)–S(3)	2.377(3)	Cu(2)–S(4)	2.2723)	S(3)–C(31)	1.793(10)
Cu(1)–N(1)	1.880(9)	Cu(2)–N(2)	1.838(12)	S(4)–C(41)	1.787(10)
Mo(1)...Cu(1)	3.653	Mo(2)...Cu(2)	3.649	Cu(1)…Cu(2)	3.147
Bond angles					
Cp(1)–Mo(1)–Cp(2)	134.2	Cu(1)–S(1)–Mo(1)	95.32(9)	Cp(3)–Mo(2)–Cp(4)	134.7
S(1)–Mo(1)–S(2)	74.10(8)	Cu(1)–S(2)–Mo(1)	98.96(10)	S(3)–Mo(2)–S(4)	74.91(9)
S(3)–Cu(1)–S(1)	98.12(10)	Cu(2)–S(3)–Mo(2)	95.70(10)	S(1)–Cu(2)–S(3)	97.52(10)
S(2)–Cu(1)–S(3)	118.38(11)	Cu(2)–S(4)–Mo(2)	98.67(11)	S(4)–Cu(2)–S(1)	115.54(11)
S(2)–Cu(1)–S(1)	79.53(9)	C(1)–N(1)–Cu(1)	168.9(12)	S(4)–Cu(2)–S(3)	80.98(10)
Cu(2)–S(1)–Cu(1)	81.10(9)	C(3)–N(2)–Cu(2)	164(2)	Cu(1)–S(3)–Mo(2)	130.09(12)
Cu(1)–S(3)–Cu(2)	81.79(10)	N(2)–C(3)–C(4)	176(2)	Cu(2)–S(1)–Mo(1)	135.00(11)
N(1)–Cu(1)–S(1)	125.7(4)	N(1)–C(1)–C(2)	178.3(14)	N(2)–Cu(2)–S(1)	105.0(5)
N(1)–Cu(1)–S(2)	124.1(3)			N(2)–Cu(2)–S(3)	124.3(5)
N(1)–Cu(1)–S(3)	106.9(3)			N(2)–Cu(2)–S(4)	128.7(5)

(Mo–S1–C11–C12 = 32°). The angles at the bridging sulphur atoms (110.87(10) and 105.51(9)°) and at the metals (S–Mo–S = 71.57(8); S–Cu–S = 71.96(8)°), as well as the Mo–Cu distance of 4.011 Å, do not suggest the existence of direct metal–metal interaction for the Mo(IV)–Cu(I) system. The S–Mo–S angle in this complex is about 2° smaller than the average bite angle of the free metalloligand (73.37°) [7].

2.2.2. Crystal structure of $[Mo(\eta^5\text{-}C_5H_5)_2(\mu\text{-}SPh)_2Cu(PPh_3)][BF_4]\cdot 0.5(Me_2CO)$ (**3**·1/2Me$_2$CO)

X-ray quality crystals of **3** were obtained, as in the previous case, by slow diffusion of diethyl ether into an acetone solution of the compound. This complex crystallises in triclinic unit cells, each containing discrete anions and cations, as well as acetone molecules in a proportion of 1 (**3**):0.5 (Me_2CO). The cation of **3** is depicted in the ORTEP drawing in Fig. 2. Selected bond distances and angles are given in Table 1. The Mo atom presents a distorted pseudotetrahedral coordination sphere similar to that found for compound **1**, but the Cu atom adopts, in the present complex, a pseudotrigonal geometry consisting of the two sulphur atoms of the metalloligand and the phosphorus atom of the bound PPh_3. The MoS_2Cu core of **3** is puckered, with an angle of 154.2° between the S1–Mo–S2 and the S1–Cu–S2 planes and a Mo–Cu distance of 3.664 Å. The substituents of the bridging thiolates present a *cis* orientation and they are out of the S1–Mo–S2 plane, with torsion angles S1–Mo–S2–C21 of 166° and S2–Mo–S1–C11 of 142°. The thiolate groups exhibit torsion angles of 67° (Mo–S1–C11–C12) and 24° (Mo–S2–C21–C22) in order to minimise steric repulsions with the closer Cp ring. The S–Mo–S angle of 72.52(6) ° is only 1° larger than the corresponding angle in complex **1**, but the S–Cu–S angle is about 8° wider and the Cu–S and Cu–P distances are shorter in **3**, as a result of the less hindered coordination environment of the Cu atom in this case.

2.2.3. Crystal structure of $[Mo(\eta^5\text{-}C_5H_5)_2(\mu\text{-}SPh)_2Cu(NCCH_3)]_2[BF_4]_2$ (7)

Crystals of **7** were obtained by anaerobic diffusion of diethyl ether into an acetonitrile solution of **7**. The X-ray crystallographic study of this compound showed the lattice is made up of orthorhombic unit cells comprised of discrete cations and anions. Fig. 3 shows an ORTEP drawing of the cation of **7**. Selected bond distances and angles are given in Table 1.

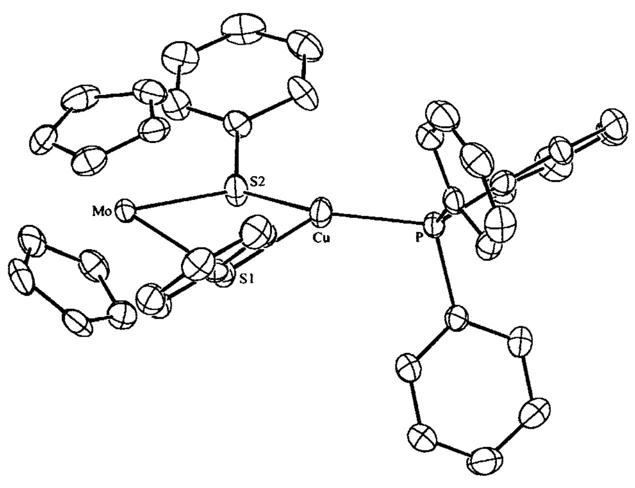

Fig. 2. ORTEP drawing of the cation $[Mo(\eta^5\text{-}C_5H_5)_2(\mu\text{-}SPh)_2Cu(PPh_3)]^+$ (**3**). Hydrogen atoms are omitted for clarity. The labelled atoms are symmetry related to their unlabelled counterparts.

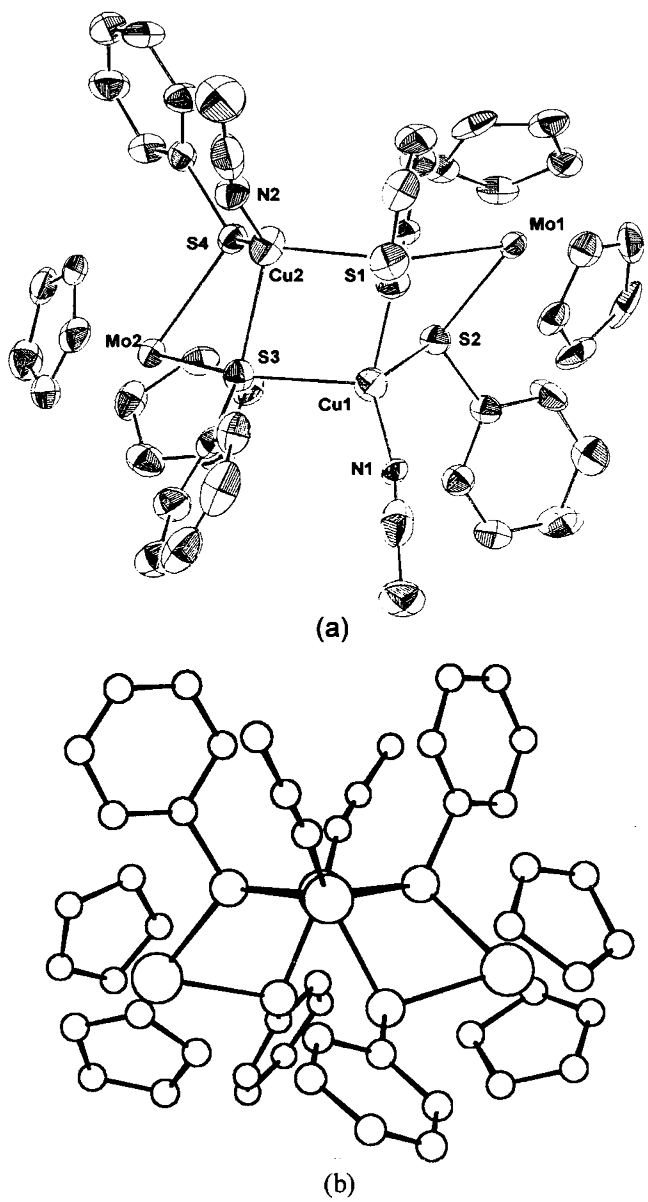

Fig. 3. (a) ORTEP drawing of the cation $[MoCp_2(\mu\text{-}SPh)_2CuNCCH_3]_2^{2+}$ (**7**). Hydrogen atoms are omitted for clarity. The labelled atoms are symmetry related to their unlabelled counterparts. (b) View along the Cu...Cu direction.

The two Mo atoms of this complex are in a distorted pseudotetrahedral environment, and the coordination sphere of the two Cu atoms is also tetrahedral. The distances found for Mo–Cp (1.97–2.00 Å) and Mo–S (2.49–2.53 Å) and the angles Cp–Mo–Cp (134–135°) are in the common range found for biscyclopentadienyl compounds. The sulphur atoms S1 and S3, coordinated to three metal atoms, exhibit longer Cu–S bond dis-

Table 2
$[MCp_2(\mu\text{-}SR)_2]$ (M = Mo(IV), Ti(IV)) and related $[MCp_2(\mu\text{-}SR)_2M'L_n]$ ELHB systems [a]

Compound	Electron count	S–M–S	S–M′–S	M–S–M′ [b]	M–M′	Ref.
$[MoCp_2(\mu\text{-}SPh)_2]$	[d^2]	73.4				[7]
$[MoCp_2(\mu\text{-}SPh)_2Cu(PPh_3)_2]^+$ (**1**)	[d^2–d^{10}]	71.6	72.0	108.2	4.01	This work
$[MoCp_2(\mu\text{-}SPh)_2Cu(PPh_3)]^+$ (**3**)	[d^2–d^{10}]	72.5	79.6	100.3	3.66	This work
$[MoCp_2(\mu\text{-}SPh)_2Cu(NCMe)]_2^{2+}$ (**7**)	[d^2–d^{10}]	74.1	81.0	95.5 (μ^3-S)	3.65	This work
		74.9	79.5	98.8 (μ^2-S)	3.65	This work
$[MoCp_2(\mu\text{-}S^tBu)_2]$	[d^2]	71.1				[8]
$[MoCp_2(\mu\text{-}S^tBu)_2NiCp]^+$	[d^2–d^8]	68.7	79.5	95.1	3.49	[3e]
$[\{MoCp_2(\mu\text{-}SMe)_2\}Ni]^{2+}$	[d^2–d^8]	70.3	82.2	92.3	3.39	[9]
$[TiCp_2(\mu\text{-}SMe)_2]$	[d^0]	93.7				[5c]
$[\{TiCp_2(\mu\text{-}SMe)_2\}Ni]$	[d^0–d^{10}]	98.6	117.4	73.1	2.79	[5c]
$[TiCp_2(\mu\text{-}SMe)_2Ru(NC^tBu)(Cp^*)]^+$	[d^0–d^6]	96.4	101.2	81.3	3.13	[5d]
$[TiCp_2(\mu\text{-}SMe)_2Mo(CO)_4]$	[d^0–d^6]	99.9	94.6	82.8	3.32	[4b]
$[\{Ti(Cp')_2(\mu\text{-}SPh)_2\}Pd(C_6F_5)]$ [c]	[d^0 – d^8]	95.7	99.7	80.9	3.14	[5f]
$[\{TiCp_2(\mu\text{-}SC{\equiv}CPh)_2\}Ni]$	[d^0–d^{10}]	98.3	117.9	72.1	2.79	[5e]
$[TiCp_2(\mu\text{-}SEt)_2]$	[d^0]	93.8				[10]
$[TiCp_2(\mu\text{-}SEt)_2Cu(NCMe)_2]^+$	[d^0–d^{10}]	99.4	112.2	73.5	2.85	[5b]
$[TiCp_2(\mu\text{-}SEt)_2Cu(PPh_3)]^+$	[d^0–d^{10}]	99.1	114.1	75.5	2.80	[5a]
$[TiCp_2(\mu\text{-}SEt)_2Cu(PCy_3)]^+$	[d^0–d^{10}]	99.1	110.9	73.5	2.84	[5a]

[a] Distances are given in Å, angles in °.
[b] Average values.
[c] (Cp′) = ($C_5H_4SiMe_3$).

tances (2.377–2.436 Å) than S2 and S4, which coordinate only two metal centres (Cu–S2 = 2.288 and Cu–S4 = 2.272 Å).

Complex **7** can be analysed as being formed by two $[MoCp_2(\mu\text{-}SPh)_2Cu(NCCH_3)]$ units, with a structure similar to **3**, linked to each other through the Cu atom and one of the S atoms (μ_3-SPh), with formation of a third core (Cu–S–Cu–S) between the two units. This ring is not considerably puckered (folding angle = 166.1°), and the acetonitrile ligands are coordinated to Cu in a *cis* arrangement (Fig. 3b). The MoS_2Cu cores are puckered with angles of 146.2° (Mo1–Cu1) and 149.4° (Mo2–Cu2), with the thiolate groups in a *cis* configuration, characterised by the angles C11–S1–S2–C21 = 12° and C31–S3–S4–C41 = 10° with S–M–S–C torsions of 153.2, 149.9, 159.2 and 142.2° for the S1Ph1, S2Ph2, S3Ph3 and S4Ph4 groups, respectively. The phenyl rings of each one of these thiolate groups are rotated relative to the Mo–S–C planes, which can be visualised by the Mo–S–C–C angles of 59.3, 38.5, 35.7 and 59.8°, respectively. The observed metal–metal distances on the three M–S–M–S cores (Mo1–Cu1 = 3.653, Mo2–Cu2 = 3.649 and Cu1–Cu2 = 3.147 Å), the Mo–S–Cu angles (95–99°) and the S–Mo–S angles (74 and 75°) are not compatible with the existence of direct metal–metal interactions in **7**, as in compounds **1** and **3**, described above.

Comparison of several structural parameters for Mo and Ti metalloligands against a number of related ELHB compounds are shown in Table 2. The (S–M–S) angles of the free $[MCp_2(SR)_2]$ bidentate ligands are considerably smaller for the Mo(IV) complexes (71.1–73.56°), which adopt an *exo* conformation, than for the Ti(IV) species (93.7–93.8°), in which the R groups are *endo*.

The bimetallic species with the $MoCp_2$ fragment (*exo*, d^2) exhibit S–Mo–S angles similar to (and generally smaller than) those observed in the corresponding free metalloligands. Even in the dimer **7**, which contains two sets of non-equivalent sulphur atoms, (two μ_3-SPh and two μ_2-SPh) the S–Mo–S′ angles are only about 1.3° larger. The Mo–S–M′ angles and the Mo–M′ distances are large and the 18 electron rule is obeyed, so the Mo atom is electronically saturated and a metal–metal bond is not likely to occur. Thus, the largest M–M′ distances, among the ELHB systems shown in Table 2, occur in the Mo(IV)–Cu(I) systems.

To the contrary, in the $TiCp_2$ derivatives (*endo*, d^0), the S–Ti–S angles open wider (about 6°) than in the free monometallic species; the Ti–S–M′ angles close down and the Ti–M′ distances are shorter. As the Ti coordination sphere is unsaturated (16 electrons), when M′ is electron-rich, a dative metal–metal bond is postulated. Thus, the shortest M–M′ distances are found in the d^0–d^{10} systems (Ti(IV)–Cu(I)/Ni(0), 2.782–2.846 Å).

The S–M–S angles in the binuclear compounds shown in Table 2 do not seem to be significantly affected by the R substituents on sulphur, either in the Ti(IV) or in the Mo(IV) derivatives.

2.3. Variable temperature studies

The ^{1}H spectra of compounds **1** and **3** were examined over the temperature range +40 to −80 °C, showing no temperature dependence of the cyclopentadienyl proton resonances. A single resonance is observed over the whole temperature range for both complexes (at 5.38 ppm for **1** and at approximately 5.60 ppm, with a slight decrease of the chemical shift at lower temperatures, for **3**), indicating the equivalence of both Cp groups in each compound. This is consistent with a *transoid* arrangement of the phenyl groups on the bridging sulphurs. Thus, in solution, even at low temperatures there is no evidence for the *cisoid* form observed in the crystals; a fast interconversion (in the NMR time scale) of *cis* and *trans* conformers may take place, averaging the signal.

In similar Ti–Cu compounds [5a,5b], a slower fluxional process takes place and the cyclopentadienyl proton resonances are temperature dependent: at higher temperatures a singlet is observed but, as the system is cooled, the signal broadens and splits into two sharp resonances, assigned to the *cisoid* conformer. However, in a similar Ti–Ru system [5d], the substituents on the sulphur maintain a *cis* conformation, even in solution, and no *cis–trans* interconversion has been observed.

3. Experimental

3.1. General procedures

All manipulations and reactions were performed under dinitrogen or Ar atmospheres using standard Schlenk-tube techniques. The NMR spectra were recorded on a Varian 300 spectrometer using $SiMe_4$ as internal reference for ^{1}H-NMR. ^{31}P-NMR spectra were recorded on the spectrometer operating at 121.4 MHz with chemical shifts referred to H_3PO_4 85% external reference. Deuterated solvents were dried over molecular sieves and degassed by the freeze–thaw method at least three times prior to use. Elemental analyses were performed by Laboratório de Análises do Instituto Superior Técnico on a Fisons Instruments 1108 spectrometer. Specific conductivities were measured on a digital conductimeter GC 855 Schott, using 10^{-3} M solutions of the complexes in nitromethane, calibrated with a KCl solution. The values were compared with those for standard electrolytes [11]. Infrared spectra were recorded on a Perkin–Elmer 683 spectrophotometer in KBr pellets.

The solvents were reagent grade, distilled from the appropriate drying agents [12] just before use, under dinitrogen. The starting materials $[MCp_2X_2]$ (M = Mo(IV), W(IV), X = Cl, SR) were prepared by reported methods [13]; $[Cu(NCCH_3)_4][BF_4]$ was prepared by the literature method [14]. Commercial $MoCl_5$, WCl_6 and PPh_3, purchased from Aldrich and PhSH, $^{t}BuSH$, NaOH and $HBF_4{\cdot}Et_2O$, purchased from Merck, were used without further purification; py was distilled over NaOH.

3.2. Syntheses

3.2.1. Preparation of compounds $[M(\eta^5\text{-}C_5H_5)_2(\mu\text{-}SR)_2CuL_2][BF_4]$ (A) (**1**–**2**)

These complexes were synthesised in a similar manner; thus, only the general preparation method is described.

To a suspension of $[Cu(NCCH_3)_4][BF_4]$ (1.0 mmol) in THF (ca. 50 ml) was added L (2.0 mmol) and the mixture was stirred for 15 min. $[M(\eta^5\text{-}C_5H_5)_2(SR)_2]$ (1.0 mmol) was then added. The solution became dark red immediately. After 3 h reaction at room temperature (r.t.), the solvent was evaporated to dryness and the solid washed with three 20-ml portions of hexane and dried under vacuum. Recrystallisation by slow diffusion of Et_2O into acetone solutions of the products afforded orange crystals of **1** suitable for X-ray diffraction analysis; an orange crystalline product was also obtained for **2**.

*3.2.1.1. $[Mo(\eta^5\text{-}C_5H_5)_2(\mu\text{-}SPh)_2Cu(PPh_3)_2][BF_4]$ (**1**).* Yield: 95%; ^{1}H-NMR [300 MHz, $(CD_3)_2CO$] δ 7.52–7.32 [30H, m, 2 $P(C_6H_5)_3$], 7.10 (10H, m, 2 SC_6H_5, 5.38 (10H, s, 2 C_5H_5); ^{31}P-NMR [121.4 MHz, $(CD_3)_2CO$] δ 0.92 (s, P). Anal. Found: C, 61.99; H, 4.34; S, 5.32. Calc. for $C_{61}H_{56}BCuF_4MoOP_2S_2$: C, 62.22; H, 4.79; S, 5.45%; molar conductivity (10^{-3} M in $MeNO_2$, Ω^{-1} cm^2 mol^{-1}) 84.6. IR [KBr, cm^{-1}]: 3105 w (ν_{CH}, Cp–H); 3040 w (ν_{CH}, Ar–H); 1570 s (Ar–H); 1470 s, 1430 s, (ν_{CC}, Cp); 1090–1010 vs, broad (BF_4); 830 m, 740 vs, 690 vs (C–H out-of-plane bends).

*3.2.1.2. $[W(\eta^5\text{-}C_5H_5)_2(\mu\text{-}SPh)_2Cu(PPh_3)_2][BF_4]$ (**2**).* Yield 90%; ^{1}H-NMR [300 MHz, $(CD_3)_2CO$] δ 7.52–7.30 [30H, m, 2 $P(C_6H_5)_3$], 7.20 (4H, m) and 7.12 (6H, m), 2 SC_6H_5, 5.38 (10H, s, 2 C_5H_5); ^{31}P-NMR [121.4 MHz, $(CD_3)_2CO$] δ 2.92 (s, P). Anal. Found: C, 56.86; H, 4.18; S, 4.05. Calc. for $C_{58}H_{50}BCuF_4P_2S_2W$: C, 57.70; H, 4.17; S, 5.31%; molar conductivity (10^{-3} M in $MeNO_2$, $\Omega^{-1}cm^2mol^{-1}$) 82.7. IR [KBr, cm^{-1}]: similar to **1**.

3.2.2. Preparation of compounds $[M(\eta^5\text{-}C_5H_5)_2(\mu\text{-}SR)_2CuL][BF_4]$ **B** (**3**–**6**)

Complexes **3**–**6**, have been prepared in a manner analogous to that used for the previous compounds, **A**, but using two equivalents of the ligand L. Recrystallisations have also been carried out as previously, affording dark red crystals of **3** suitable for X-ray diffraction analysis; red crystals of **4**, and clean brown–red powders of **5** and **6**.

*3.2.2.1. [Mo(η^5-C_5H_5)$_2$(μ-SPh)$_2$Cu(PPh_3)][BF_4] (**3**).* Yield 90%; ^{1}H-NMR [300 MHz, $(CD_3)_2CO$] δ 7.59 [15H, m, $P(C_6H_5)_3$], 7.17 (6H, m) and 7.01 (4H, m), 2 SC_6H_5, 5.63 (10H, s, 2 C_5H_5); ^{31}P-NMR [121.4 MHz, $(CD_3)_2CO$] δ 5.6 (s, P). Anal. Found: C, 55.46; H, 4.30; S, 7.32. Calc. for $C_{40}H_{35}BCuF_4MoPS_2$: C, 56.05; H, 4.12; S, 7.48%; molar conductivity (10^{-3} M in $MeNO_2$, Ω^{-1} cm^2 mol^{-1}) 87.5. IR [KBr, cm^{-1}]: similar to **1**.

*3.2.2.2. [W(η^5-C_5H_5)$_2$(μ-SPh)$_2$Cu(PPh_3)][BF_4] (**4**).* Yield 90%; ^{1}H-NMR [300 MHz, $(CD_3)_2CO$] δ 7.61 {15H, m, $P(C_6H_5)_3$, 7.29 (4H, m) and 7.09 (6H, m), 2 SC_6H_5, 5.59 (10H, s, 2 C_5H_5); ^{31}P-NMR [121.4 MHz, $(CD_3)_2CO$] δ 5.60 (s, P); molar conductivity (10^{-3} M in $MeNO_2$, Ω^{-1} cm^2 mol^{-1}) 84.0. IR [KBr, cm^{-1}]: similar to **1**.

*3.2.2.3. [Mo(η^5-C_5H_5)$_2$(μ-SPh)$_2$Cu(NC_5H_5)][BF_4] (**5**).* Yield 30%; ^{1}H-NMR [300 MHz, $(CD_3)_2CO$] δ 8.90 (2H, m), 8.35 (1H, m) and 7.88 (2H, m), NC_5H_5, 7.37 (4H, m) and 7.11 (6H, m), 2 C_6H_5, 5.63 (10H, s, 2 C_5H_5). Anal. Found: C, 46.38; H, 3.75; N, 1.78; S, 9.39. Calc. for $C_{27}H_{25}NBCuF_4MoS_2$: C, 48.12; H, 3.74; N, 2.08; S, 9.51%. IR [KBr], (cm^{-1}): 3105 w (ν_{CH}, Cp–H); 3040 w (ν_{CH}, Ar–H); 1600 m (ν_{CN} py), 1575 m (Ar–H); 1465 m, 1440 s, (ν_{CC}, Cp); 1090–1010 vs, broad (BF_4); 835 m, 740 s, 690 s (C–H out-of-plane bends).

*3.2.2.4. [Mo(η^5-C_5H_5)$_2$(μ-S^{t}Bu)$_2$Cu(PPh_3)][BF_4] (**6**).* Yield 40%; ^{1}H-NMR [300 MHz, $(CD_3)_2CO$] δ 7.55 [15H, m, $P(C_6H_5)_3$], 5.80 (10H, s, 2 C_5H_5), 1.23 (18H, s, 2 C_4H_9); ^{31}P-NMR [121.4 MHz, $(CD_3)_2CO$] δ_P 6.85 (s, P). Anal. Found: C, 51.80; H, 4.98; S, 6.45. Calc. for $C_{38}H_{43}BCuF_4MoPS_2$: C, 54.15; H, 5.15; S, 7.59%; molar conductivity (10^{-3} M in $MeNO_2$, Ω^{-1} cm^2 mol^{-1}) 78.6. IR [KBr], (cm^{-1}): 3105 w (ν_{CH}, Cp–H); 3040 w (ν_{CH}, Ar–H); 2980 w, 2960 w, 2940 w, 2925 w (ν_{CH}, ^{t}Bu); 1480 m, 1460 m (ν_{CC}, Cp); 1455 m (ν_{PC}) 1100–1000 vs, broad (BF_4); 820 m, 745 s, 695 vs, (C–H out-of-plane bends); 520 s (PPh_3).

*3.2.3. Preparation of [Mo(η^5-C_5H_5)$_2$(μ-SPh)Cu($NCCH_3$)]$_2$[BF_4]$_2$ (**7**)*

[Mo(η^5-C_5H_5)$_2$(SPh)$_2$] (0.54 g, 1.21 mmol) was added to a stirred solution of [Cu($NCCH_3$)$_4$][BF_4] (0.20 g, 0.63 mmol) in dry MeCN (ca. 30 cm^3) and the orange–red mixture was heated at reflux temperature for 2 h. The solution was filtered and the solvent evaporated to dryness under vacuum. An orange–red solid was obtained (ca. 0.30 g, 75%). Recrystallisation by slow diffusion of Et_2O in an MeCN solution of the product afforded some dark red crystals of **7** suitable for X-ray diffraction analysis. ^{1}H-NMR (300 MHz, CD_3CN) δ 7.31 (8H, m) and 7.16 (12H, m), 4 C_6H_5], 5.35 (20 H, s, 4 C_5H_5), 1.95 (6 H, s, 2 CH_3CN); ^{1}H-NMR [300 MHz, $(CD_3)_2CO$] δ 7.42 (8 H, m) and 7.13 (12 H, m), 4 C_6H_5, 5.62 (20H, s, 4 C_5H_5), 2.09 (6H, s, 2 CH_3CN). Anal. Found: C, 47.40; H, 3.64; N, 0.08;[1] S, 10.70. Calc. for $C_{48}H_{46}N_2B_2Cu_2F_8Mo_2S_4$: C, 45.53; H, 3.65; N, 2.20; S, 10.08, 9.03%; molar conductivity (10^{-3} M in $MeNO_2$, Ω^{-1} cm^2 mol^{-1}) 138.5. IR [KBr], (cm^{-1}): 3105 w (ν_{CH}, Cp–H); 3040 w (ν_{CH}, Ar–H); 2315 vw (ν_{CN}, CH_3CN); 1570 s (Ar–H); 1470 s, 1430 s, 1415 w (ν_{CC}, Cp); 1080–1000 vs (BF_4); 830 s (ν_{CH}, Cp); 740 s, 690 vs, (C–H out-of-plane bends).

*3.2.4. Preparation of [{Mo(η^5-C_5H_5)$_2$(μ-SPh)$_2$}$_2$Cu][BF_4] (**8**)*

A solution of [Cu($NCCH_3$)$_4$][BF_4] (0.18 g, 0.57 mmol) in MeCN (ca. 20 cm^3) was added dropwise to a suspension of [Mo(η^5-C_5H_5)$_2$(SPh)$_2$] (0.50 g, 1.13 mmol) in the same solvent (ca. 30 cm^3), with stirring. After reaction at r.t. for 1 h, the resulting solution was separated from a viscous residue by filtration. Removal of solvent under vacuum afforded a dark red viscous oil. Trituration with three 20-ml portions of degassed Et_2O, followed by decantation of the solvent and evaporation of the final residual solvent, yielded a solid product which was recrystallised from MeCN by slow addition of Et_2O, affording a microcrystalline orange–reddish product (ca. 0.49 g, 85%). ^{1}H-NMR [300 MHz, CD_3CN] δ 7.28 (8H, m) and 7.09 (12H, m), 4 C_6H_5, 5.34 (20H, s, 4 C_5H_5). Anal. Found: C, 49.81; H, 3.87; S, 11.95. Calc. for $C_{44}H_{40}BCuF_4Mo_2S_4$ requires: C, 50.85; H, 3.88; S, 12.34%; molar conductivity (10^{-3} M in $MeNO_2$, Ω^{-1} cm^2 mol^{-1}) 86.2. IR [KBr], (cm^{-1}): 3105 w (ν_{CH}, Cp); 3040 w (ν_{CH}, Ph); 1575 s (Ar–H); 1470 s, 1430 s, 1415 m (ν_{CC}, Cp); 1080–1000 vs (BF_4); 830 s (ν_{CC}, Cp); 745 s, 695 s, (C–H out-of-plane bends).

3.3. X-ray diffraction study

The diffraction experiments were performed on an Enraf–Nonius TURBO CAD4 diffractometer equipped with a rotating anode, using graphite-monochromatised Mo–K_α radiation ($\lambda = 0.71069$ Å). All data were collected at 293(2) K. Using the CAD4 software, data were corrected for Lorentz and polarisation effects and empirically for absorption.

The structures were solved by Patterson methods with all non-hydrogen atoms located by successive difference Fourier synthesis. Hydrogen atoms were inserted in calculated positions and allowed to ride at fixed distances of the parent carbon atom. Further details can be seen in Table 3. Lists of the observed and

[1] Some discrepancies affecting mostly N-containing compounds have been observed, with no apparent explanation. In this case, the product was pure and crystalline and MeCN was detected in the ^{1}H-NMR spectra and in the X-ray diffraction analysis.

Table 3
Crystal data and structure refinement

Compound	$1\cdot(CH_3)_2CO$	$3\cdot1/2(CH_3)_2CO$	7
Empirical formula	$C_{61}H_{50}BCuF_4MoOP_2S_2$	$C_{41.5}H_{38}BCuF_4MoO0.5PS_2$	$C_{48}H_{46}B_2Cu_2F_8Mo_2N_2S_4$
Formula weight	1171.36	886.10	1271.69
Colour	Orange	Red	Red
Crystal system	Triclinic	Triclinic	Orthorhombic
Space group	$P\bar{1}$	$P\bar{1}$	*Pbca*
Unit cell dimensions			
a (Å)	13.152(2)	10.148(2)	13.6280(10)
b (Å)	14.712(2)	13.660(2)	20.065(2)
c (Å)	15.380(2)	14.221(2)	37.627(5)
α (°)	88.340(10)	84.580(10)	90
β (°)	70.610(10)	85.460(10)	90
γ (°)	86.550(10)	76.100(10)	90
V (Å^3)	2801.9(7)	1901.8(5)	10289(2)
Z	2	2	8
D_{calc} (Mg m^{-3})	1.388	1.547	1.642
Absorption coefficient (mm^{-1})	0.788	1.092	1.519
$F(000)$	1196	900	5088
μ(Mo–K$_\alpha$) (cm^{-1})	7.88	10.92	15.19
θ Range for data collection (°)	1.64–24.99	1.54–27.96	1.85–24.96
Index ranges	$-15\leq h\leq 0$; $-17\leq k\leq 17$; $-18\leq l\leq 17$	$-13\leq h\leq 13$; $-18\leq k\leq 18$; $-2\leq l\leq 18$	$-3\leq h\leq 16$; $-23\leq k\leq 2$; $-5\leq l\leq 44$
Reflections collected	10 328	10 964	14 399
Independent reflections	9855 [$R_{int}=0.0161$]	9145 [$R_{int}=0.1189$]	9010 [$R_{int}=0.0608$]
Refinement method	Full-matrix least-squares on F^2	Full-matrix least-squares on F^2	Full-matrix least-squares on F^2
Data/restraints/parameters	9829/10/619	7806/7/502	8962/0/727
Goodness-of-fit on F^2	1.122	1.070	1.165
Final R indices [$I>2\sigma(I)$]	$R_1=0.0908$, $wR_2=0.2126$	$R_1=0.0833$, $wR_2=0.1702$	$R_1=0.0578$, $wR_2=0.0898$
R indices (all data)	$R_1=0.1248$, $wR_2=0.2342$	$R_1=0.1533$, $wR_2=0.2312$	$R_1=0.1707$, $wR_2=0.2361$
Largest difference peak and hole (e Å^{-3})	0.931 and -0.748	1.873 and -0.490	0.578 and -0.516

calculated structure factors, tables of anisotropic thermal parameters, hydrogen atomic coordinates, bond lengths and angles and inter and intra molecular contact distances are available as supplementary material.

The structure solutions were done with SHELXS 86 [15], the refinements were carried out with SHELXL 93 [16] and the illustrations were drawn with ORTEP-II [17].

4. Supplementary material

Crystallographic data for the structural analysis have been deposited with the Cambridge Crystallographic Data Centre, CCDC nos. 158080 for (C61 H50 B1 Cu1 F4 Mo1 O1 P2 S2) (**1**·$(CH_3)_2CO$); 158079 for (C41.50 H38 B1 Cu1 F4 Mo1 O0.50 P1 S2), (**3**·1/2$(CH_3)_2CO$) and 158081 for (C48 H46 B2 Cu2 F8 Mo2 N2 S4), (**7**). Copies of this information may be obtained free of charge from The Director, CCDC, 12 Union Road, Cambridge CB2 1EZ, UK (Fax: +44-1233-336033; e-mail: deposit@ccdc.cam.ac.uk or www: http://www.ccdc.cam.ac.uk).

References

[1] (a) N. Wheatley, P. Kalck, Chem. Rev. 99 (1999) 3379;
(b) D.W. Stephan, Coord. Chem. Rev. 95 (1989) 41;
(c) M.J. Chetcuty, in: E.W. Abel, F.G.A. Stone, G. Wilkinson (Eds.), Comprehensive Organometallic Chemistry II, vol. 10, Pergamon Press, New York, 1994, pp. 23–84.

[2] (a) S.J. Tauster, C.S. Fung, R.L. Garten, J. Am. Chem. Soc. 100 (1978) 170;
(b) J.P. Belzunegui, J. Sanz, J.M. Rojo, J. Am. Chem. Soc. 114 (1992) 6749;
(c) G.J. Blyholder, J. Mol. Cat. A 119 (1997) 11.

[3] (a) A.R. Dias, M.L.H. Green, Chem. Commun. (1969) 962;
(b) A.R. Dias, M.L.H. Green, J. Chem. Soc. A (1971) 1951;
(c) A.R. Dias, M.L.H. Green, J. Chem. Soc. A (1971) 2807;
(d) T.S. Cameron, C.K. Prout, Chem. Commun. (1971) 161;
(e) H. Werner, B. Ulrich, U. Schubert, P. Hofmann, B. Zimmer-Gasser, J. Organomet. Chem. 297 (1985) 27;
(f) M.A.A.F. de, C.T. Carrondo, A.R. Dias, M.H. Garcia, P. Matias, M.F.M. Piedade, M.J. Villa de Brito, J. Organomet. Chem. 466 (1994) 159.

[4] (a) P.S. Braterman, V.A. Wilson, K.K. Joshi, J. Chem. Soc. A (1971) 191;
(b) G.R. Davies, B.T. Kilbourn, J. Chem. Soc. A (1971) 87.

[5] (a) T.W. Wark, D.W. Stephan, Inorg. Chem. 26 (1987) 363;
(b) T.W. Wark, D.W. Stephan, Inorg. Chem. 29 (1990) 1731;
(c) T.W. Wark, D.W. Stephan, Organometallics 8 (1989) 2836;
(d) K. Fujita, M. Ikeda, Y. Nakano, T. Kondo, T. Mitsudo, J. Chem. Soc. Dalton. Trans. (1998) 2907;

(e) H. Sugiyama, Y. Hayashi, H. Kawaguchi, K. Tatsumi, Inorg. Chem. 37 (1998) 6773;
(f) U. Amador, E. Delgado, J. Forniés, E. Hernandez, E. Lalinde, M.T. Moreno, Inorg. Chem. 34 (1995) 5279.
[6] (a) M.J. Calhorda, A. Galvão, in: M. Gielen (Ed.), Topics in Physical Organometallic Chemistry, Freud Publishing House, Tel Aviv, 1992, pp. 93–138;
(b) R. Rousseau, D. Stephan, Organometallics 10 (1991) 3399.
[7] A.R. Dias, M.H. Garcia, M.F.M. Piedade, M.A.A.F. de C.T. Carrondo, J. Organomet. Chem 632 (2001) 107–112.
[8] M.A.A.F. de C.T. Carrondo, P.M. Matias, G.A. Jeffrey, Acta Crystallogr. Sect. C 40 (1984) 932.
[9] K. Prout, S.R. Kritchley, G.V. Rees, Acta Crystallogr. Sect. B 30 (1974) 2305.
[10] M.J. Calhorda, M.A.A.F. de C.T. Carrondo, A.R. Dias, C.F. Frazão, M.B. Hursthouse, J.A. Martinho Simões, C. Teixeira, Inorg. Chem. 27 (1988) 2513.
[11] W.J. Geary, Coord. Chem. Rev. 7 (1971) 81.
[12] D.D. Perrin, W.L.F. Amarego, D.R. Perrin, Purification of Laboratory Chemicals, 2nd edn, Pergamon, New York, 1980.
[13] (a) M.G. Harriss, M.L.H. Green, W.E. Lindsell, J. Chem. Soc. A (1969) 1453;
(b) M.L.H. Green, W.E. Lindsell, J. Chem. Soc. A. (1967) 1455;
(c) R.L. Cooper, M.L.H. Green, J. Chem. Soc. A (1967) 1155;
(d) M.L.H. Green, P.J. Knowles, J. Chem. Soc. Perkin Trans. I (1973) 989.
[14] G.J. Kubas, Inorg. Synth. 19 (1979) 90.
[15] G.M. Sheldrick, SHELXS 86; Crystallographic Calculation Program, University of Cambridge, 1986.
[16] G.M. Sheldrick, SHELXL 93; Crystallographic Calculation Program, University of Cambridge, UK, 1993.
[17] C.K. Johnson, ORTEP-II, Report ORNL-5138, Oak Ridge National Laboratory, Park Ridge, TN, 1976.